Supplementary information

Isolating Cu-Zn active-sites in Ordered Intermetallics to Enhance Nitrite-to-Ammonia Electroreduction

Jiao Lan[1, 3], Zhen Wang[1, 3], Cheng-wei Kao[2], Ying-Rui Lu[2], Feng Xie[1], Yongwen Tan[1*]

[1] College of Materials Science and Engineering, Hunan University, Changsha, Hunan 410082, China.

[2] National Synchrotron Radiation Research Center, Hsinchu 300092, Taiwan.

[3] Jiao Lan and Zhen Wang contributed equally to this work

*e-mail: tanyw@hnu.edu.cn

Table of Contents

concentrations of NO_2^- ranging from 1mM to 1 M.

25. Supplementary Fig. 25| NO_2^--N concentration in solution after MEA test.

26. Supplementary Fig. 26| Morphology and composition of np/ISAA-CuZn after MEA test.

27. Supplementary Fig. 27| Optical photograph of the tailor-made electrolytic cell used. for in situ XAS characterization.

28. Supplementary Fig. 28| In situ XAS measurements of np/Cu at different applied potentials.

29. Supplementary Fig.29| Optical photograph of the tailor-made electrolytic cell used. for in situ ATR-SEIRAS characterization.

30. Supplementary Fig. 30| Reaction pathway of the NO_2RR and adsorption models of intermediates on Cu (111) surfaces.

31. Supplementary Fig. 31| Reaction pathway of the NO_2RR and adsorption models of intermediates on $CuZn_4$ surfaces.

32. Supplementary Fig. 32| Reaction pathway of the NO_2RR and adsorption models of intermediates on Cu_5Zn_8 surfaces.

33. Supplementary Fig. 33| Reaction pathway of the NO_2RR and adsorption models of intermediates on ISAA-CuZn surfaces.

34. Supplementary Fig. 34| Modelling of adsorption of *NOOH and *HNOO intermediates on Cu, $CuZn_4$, Cu_5Zn_8 and ISAA-CuZn surfaces, respectively.

35. Supplementary Fig. 35| The relationship between computational ε and ΔG of $*NO_2$ protonation.

36. Supplementary Fig. 36| Calculated of the water dissociation step on Cu and np/ISAA-CuZn surfaces.

37. Supplementary Table 1 ICP-OES test result.

38. Supplementary Table 2 EXAFS fitting parameters.

39. Supplementary Table 3 Total energy and free energy correction value.

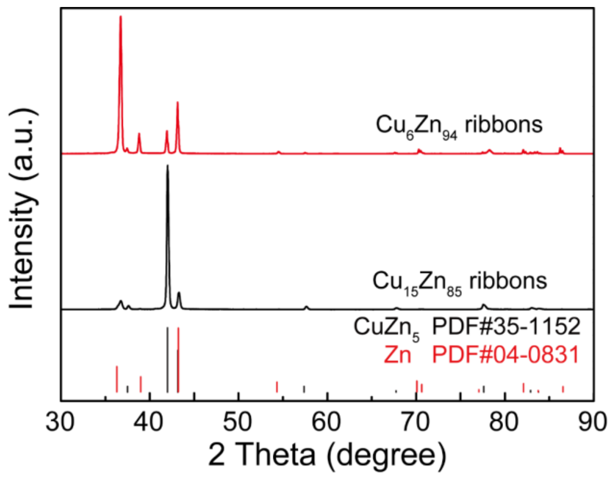

Supplementary Fig. 1| XRD spectra of Cu_6Zn_{94} and $Cu_{15}Zn_{85}$ ribbons.

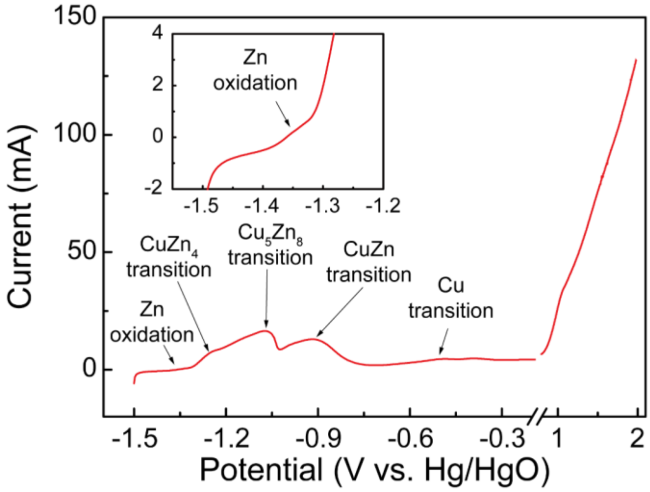

Supplementary Fig. 2| The LSV curve of the $Cu_{15}Zn_{85}$ ribbons in 1 M KOH.

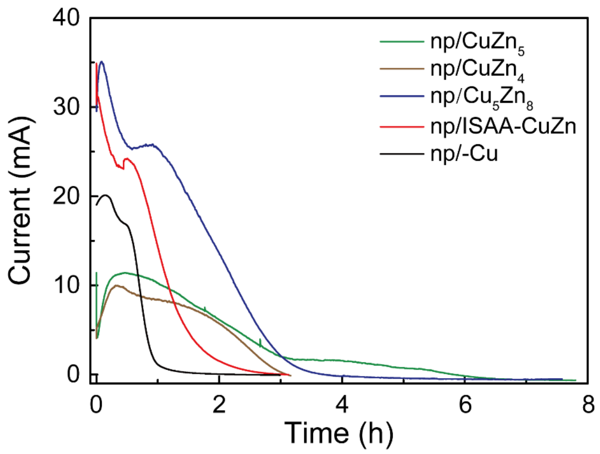

Supplementary Fig. 3| The chronoamperometry curves of np/$CuZn_5$, np/$CuZn_4$, np/Cu_5Zn_8, np/ISAA-CuZn, and np/Cu at the corresponding voltages.

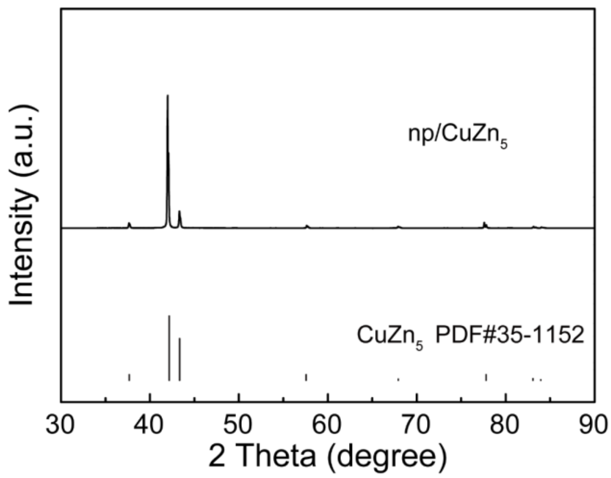

Supplementary Fig. 4| XRD spectra of np/$CuZn_5$.

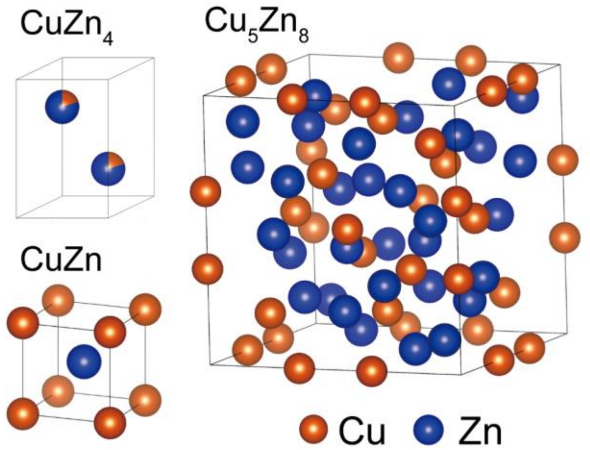

Supplementary Fig. 5| Crystal structure of Cu-Zn IMCs.

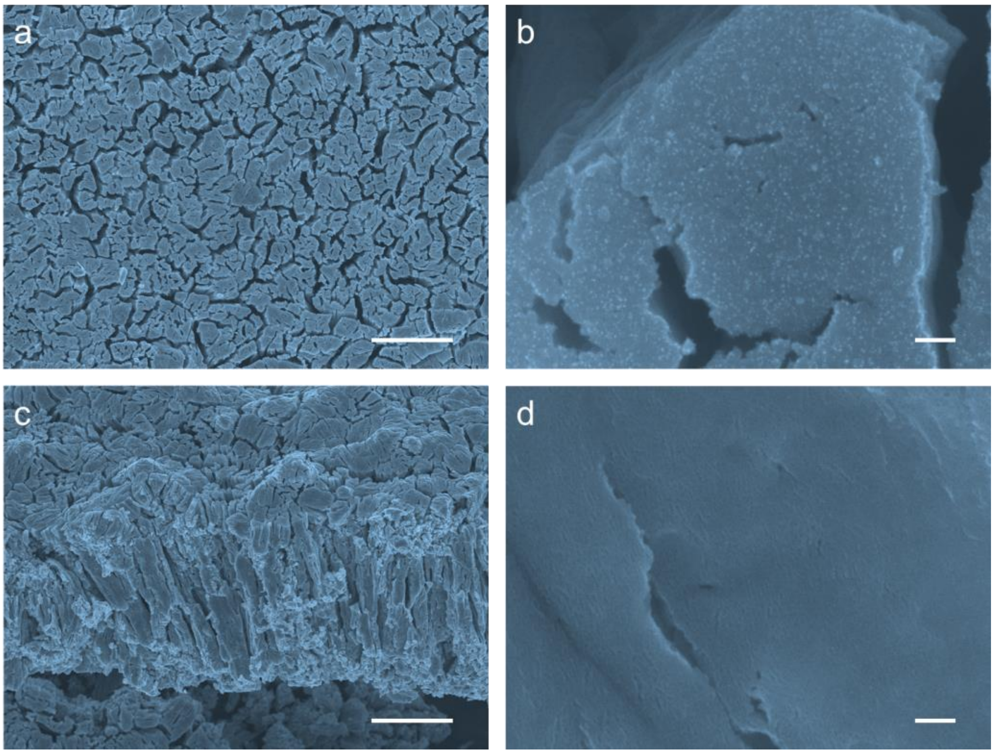

Supplementary Fig. 6| SEM images of np/$CuZn_4$. Scale bars: **a**, **c** 10 μm, **b**, **d** 100 nm.

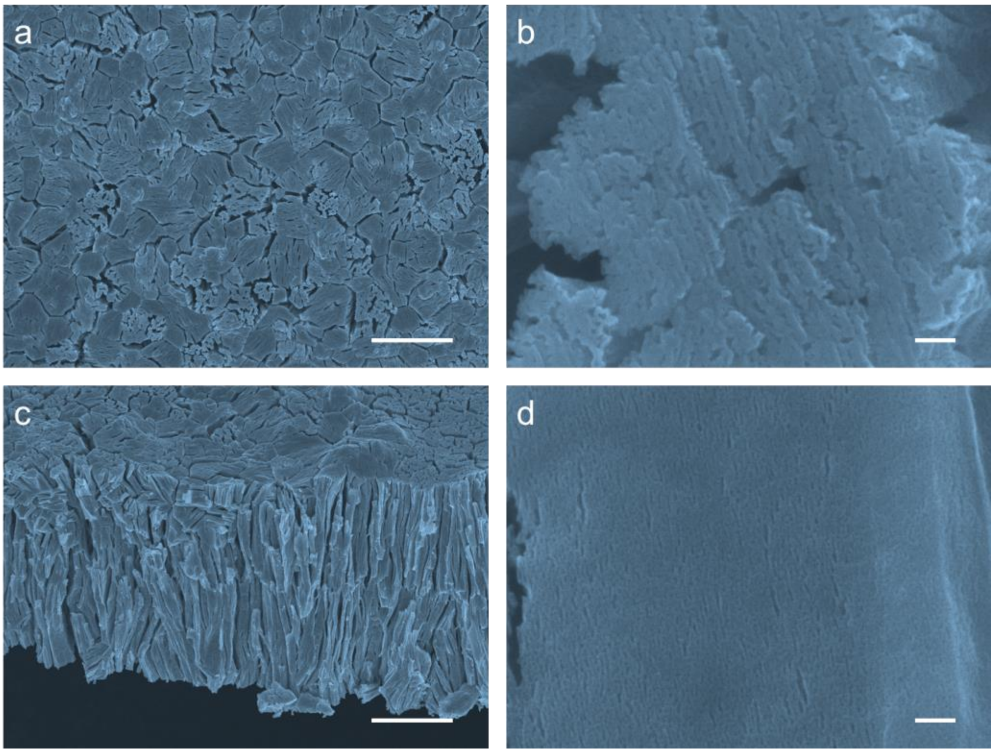

Supplementary Fig. 7| SEM images of np/Cu_5Zn_8. Scale bars: **a**, **c** 10 μm, **b**, **d** 100 nm.

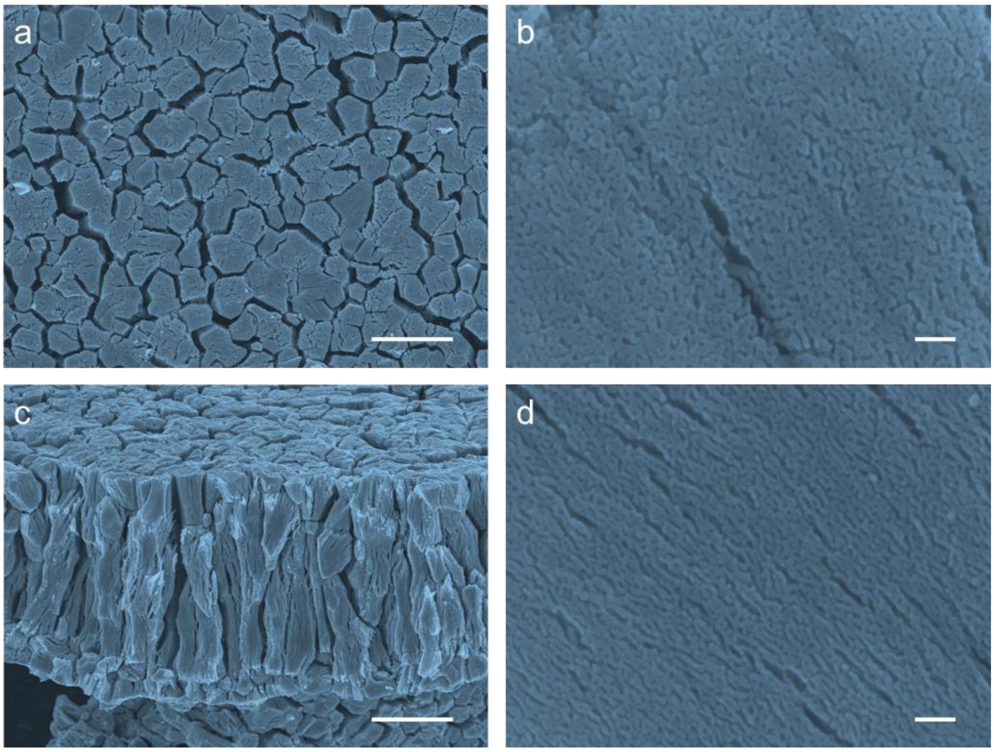

Supplementary Fig. 8| SEM images of np/ISAA-CuZn. Scale bars: **a**, **c** 10 μm, **b**, **d** 100 nm.

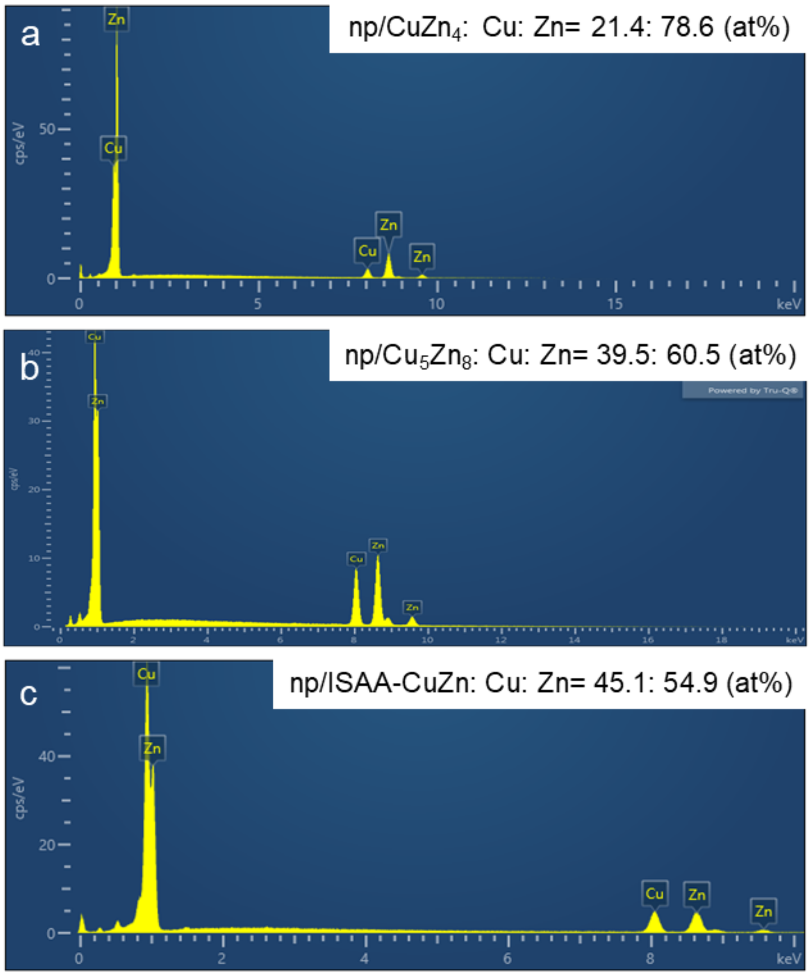

Supplementary Fig. 9| SEM-EDS test results. EDS spectroscopy and corresponding element content of np/$CuZn_4$ (**a**), np/Cu_5Zn_8 (**b**), np/ISAA-CuZn (**c**).

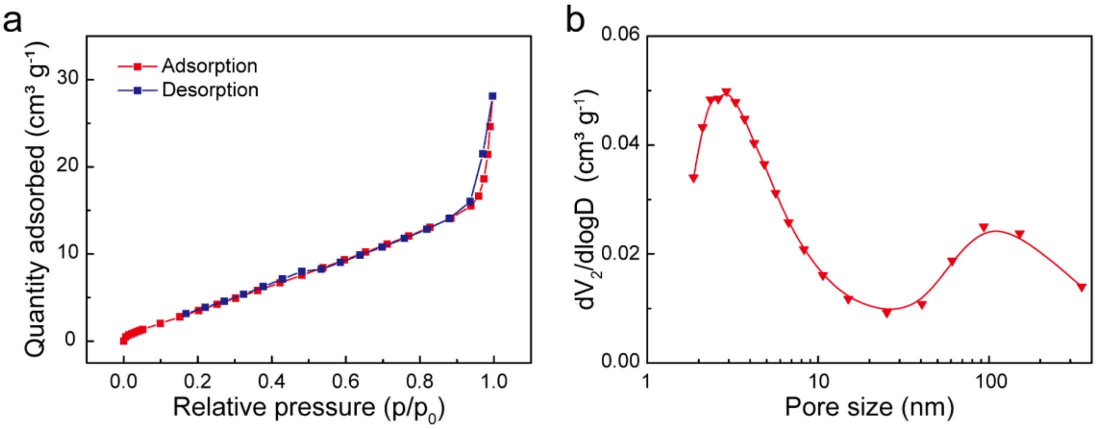

Supplementary Fig. 10| The results of BET test. Nitrogen adsorption/desorption curves (**a**) and pore size distribution (**b**) of np/ISAA-CuZn.

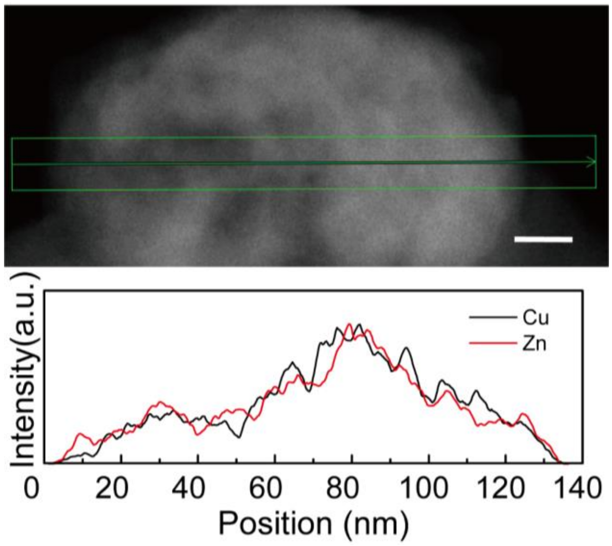

Supplementary Fig. 11| EDS composition line diagrams of np/ISAA-CuZn. Scale bar: 5 nm.

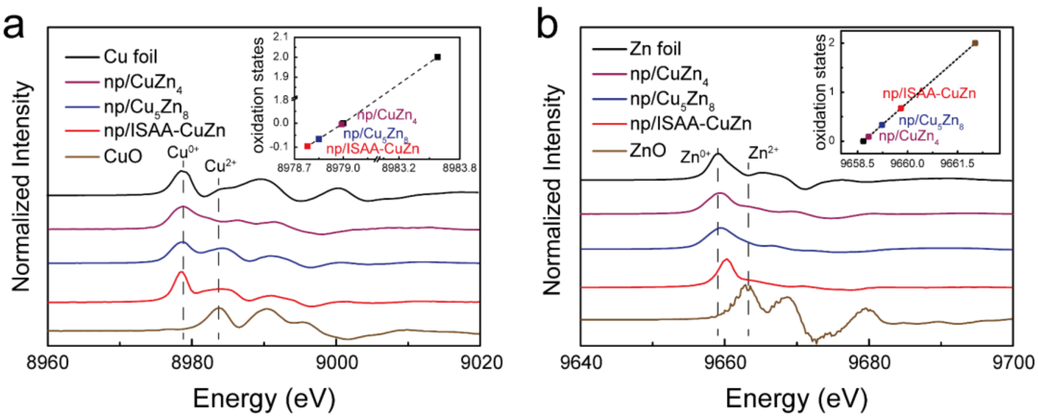

Supplementary Fig. 12| The fitted average oxidation states. a, The first derivatives of the Cu K-edge XANES spectra of of np/$CuZn_4$, np/Cu_5Zn_8, np/ISAA-CuZn, Cu foil, and CuO, insert: average oxidation states of Cu. **b,** The first derivatives of the Zn K-edge XANES spectra of of np/$CuZn_4$, np/Cu_5Zn_8, np/ISAA-CuZn, Zn foil, and ZnO, insert: average oxidation states of Zn.

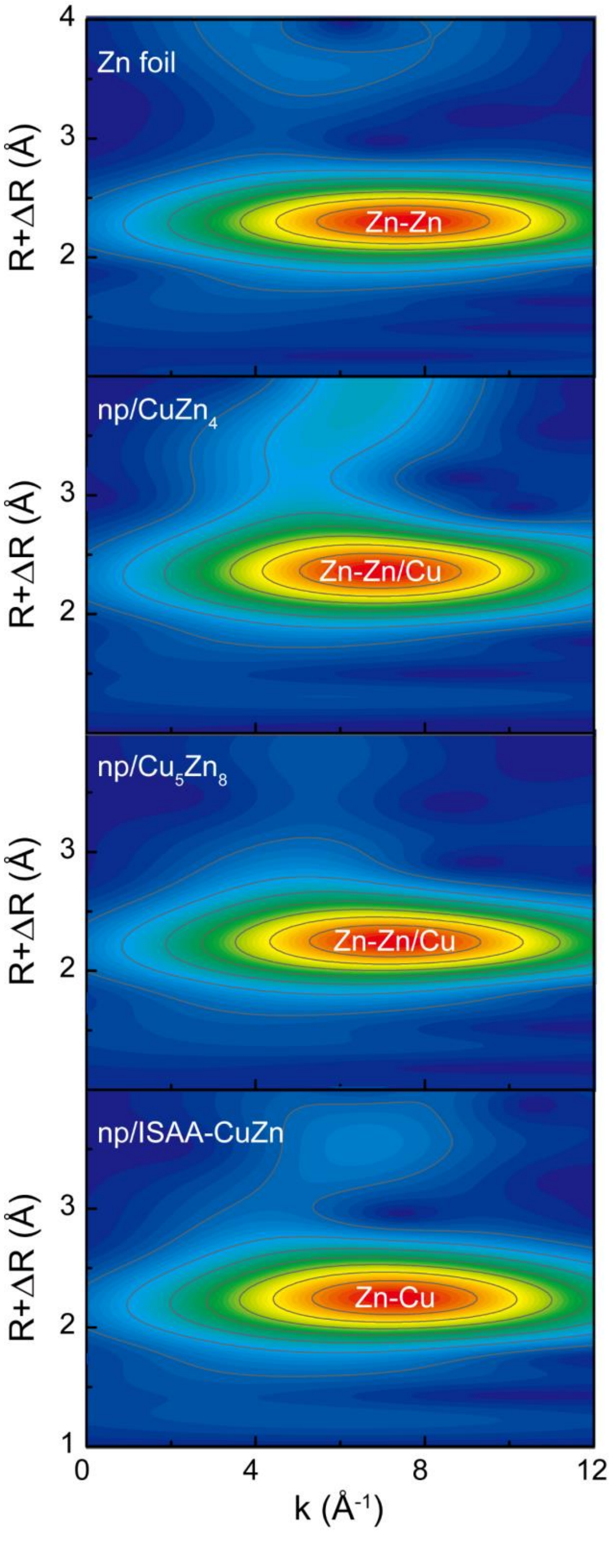

Supplementary Fig. 13| WT-EXAFS spectra. The Zn K-edge WT-EXAFS spectra of np/$CuZn_4$, np/Cu_5Zn_8, np/ISAA-CuZn, and Zn foil.

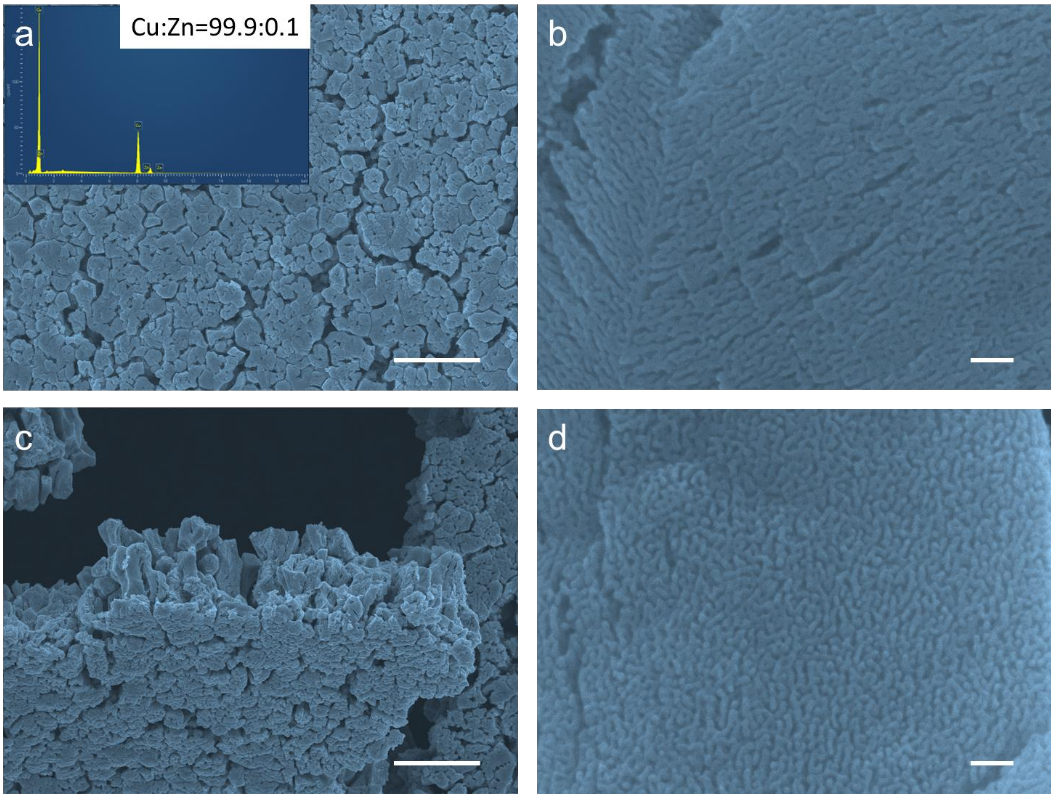

Supplementary Fig. 14| SEM images of np/Cu. Insert of (**a**): Corresponding SEM-EDS elemental distributions. Scale bars: **a**, **c** 10 μm, **b**, **d** 100 nm.

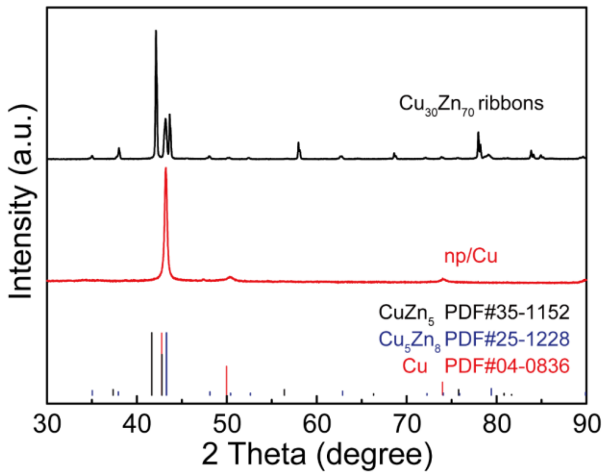

Supplementary Fig. 15| XRD spectra of $Cu_{30}Zn_{70}$ ribbons and np/Cu.

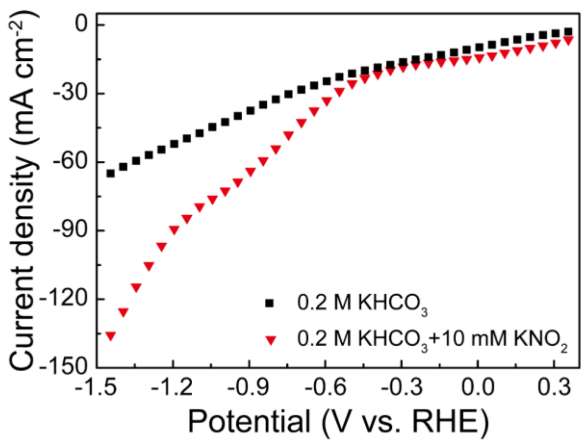

Supplementary Fig. 16| LSV curves. LSV curves of np/ISAA-CuZn in 0.2 M $KHCO_3$ with or without 10 mM of NO_2^-.

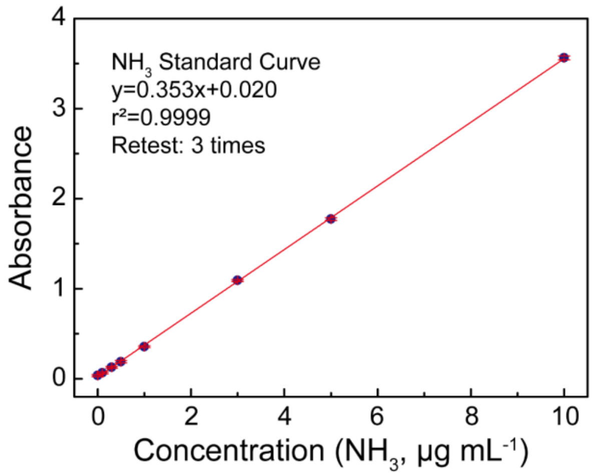

Supplementary Fig. 17| Calibration curve used for estimation of NH_3.

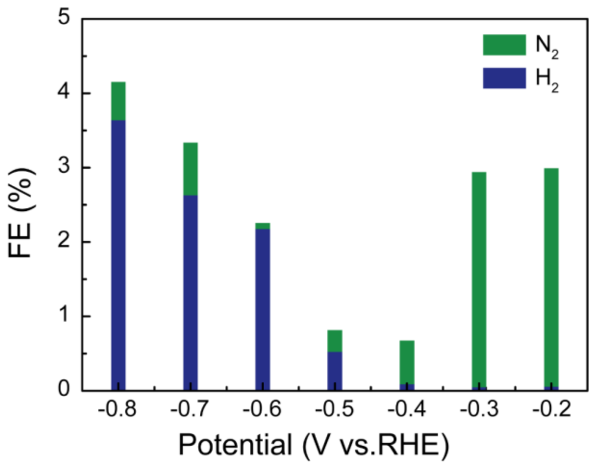

Supplementary Fig. 18| The H_2 and N_2 FE of np/ISAA-CuZn at -0.2 - -0.8 V vs. RHE in 0.2 M $KHCO_3$ + 10 mM KNO_2.

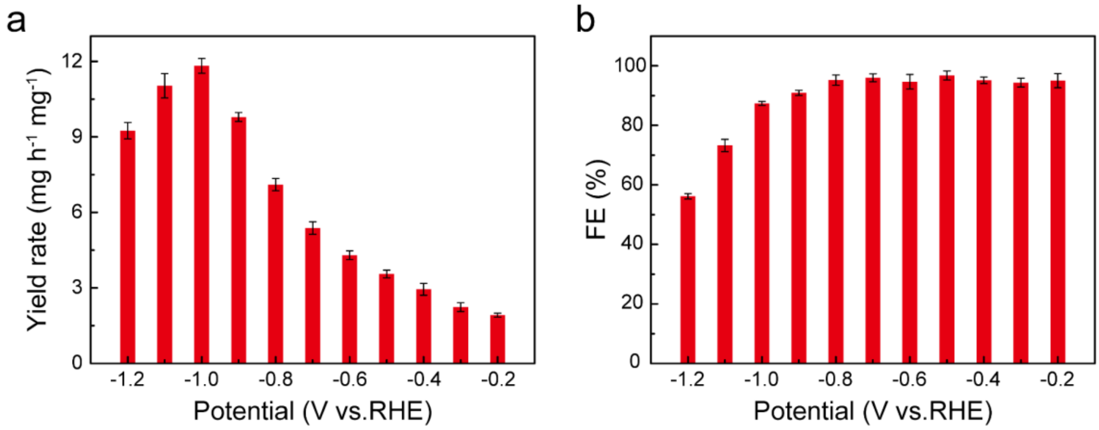

Supplementary Fig. 19| The NH_3 yield rate and FE of np/ISAA-CuZn. The NH_3 yield rate (**a**), and FE (**b**) of np/ISAA-CuZn at -0.2 - -1.2 V vs. RHE in 0.2 M $KHCO_3$ + 10 mM KNO_2. The error bands represent the standard deviation of the data obtained from more than three repetitions.

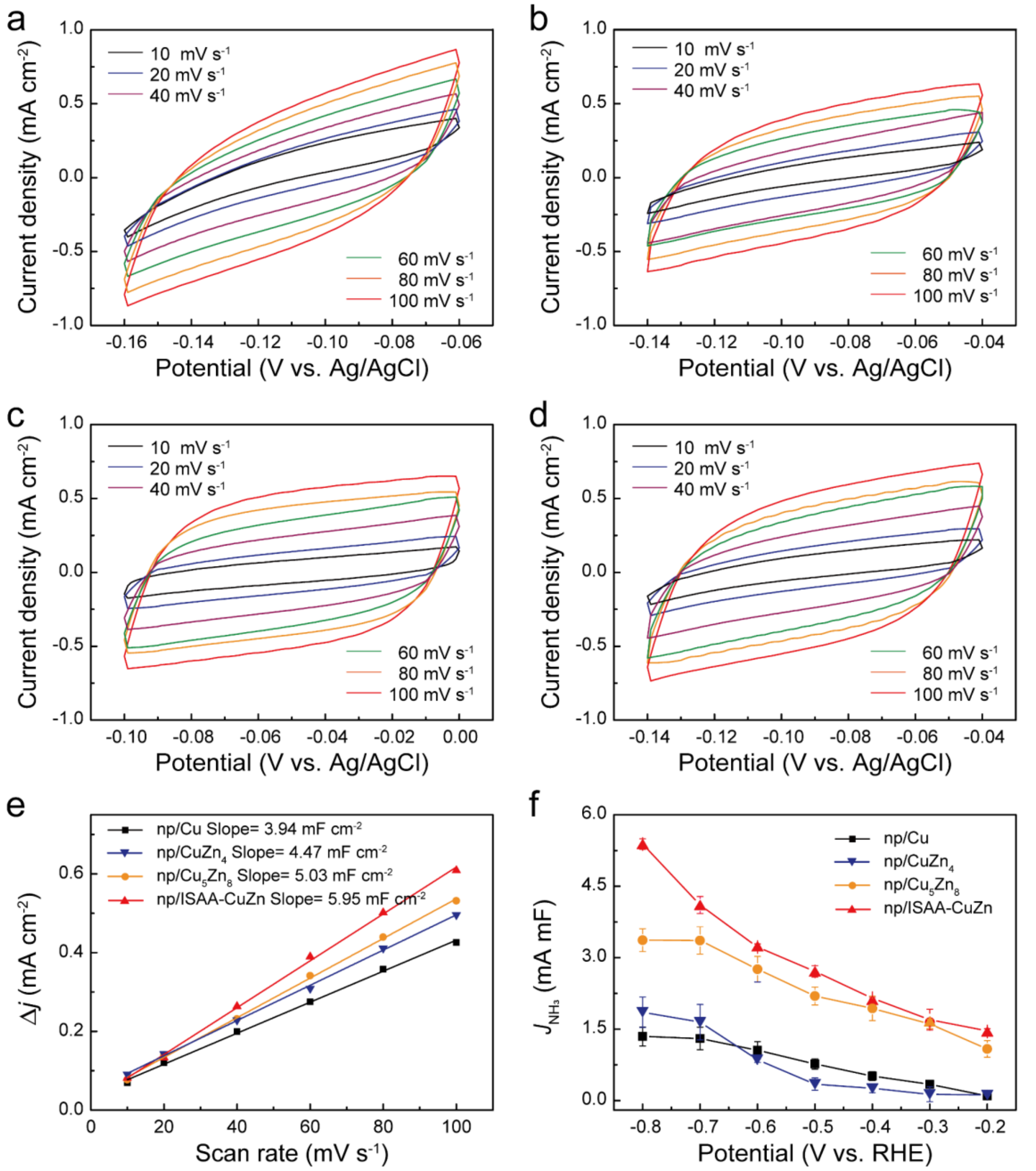

Supplementary Fig. 20| Evaluation of intrinsic activity of different catalysts. Cyclic voltammograms for **a**, np/Cu, and **b**, np/$CuZn_4$, **c**, np/Cu_5Zn_8, **d**, np/ISAA-CuZn. **e**, Plots of the current density versus the scan rate for np/Cu, np/$CuZn_4$, np/Cu_5Zn_8 and np/ISAA-CuZn. **f**, ECSA-normalized NH_3 current density under different potential of np/Cu, np/$CuZn_4$, np/Cu_5Zn_8 and np/ISAA-CuZn.

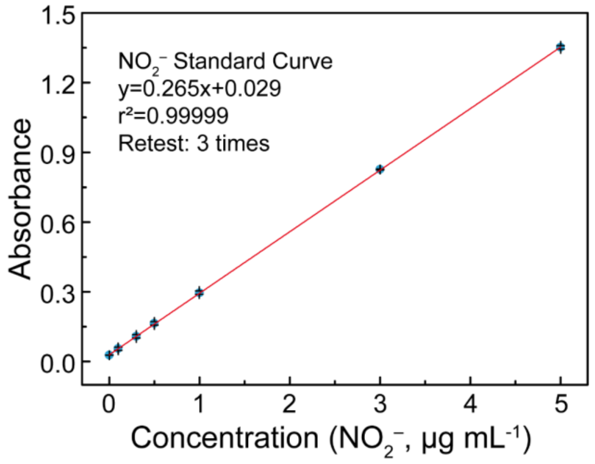

Supplementary Fig. 21| Calibration curve used for estimation of NO_2^-.

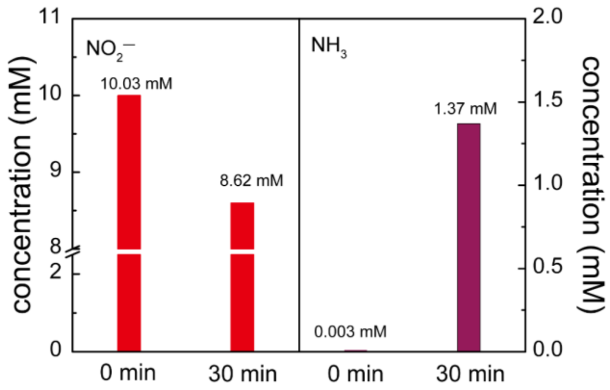

Supplementary Fig. 22| NO_2^- concentration before and after reaction at -0.5 V vs. RHE.

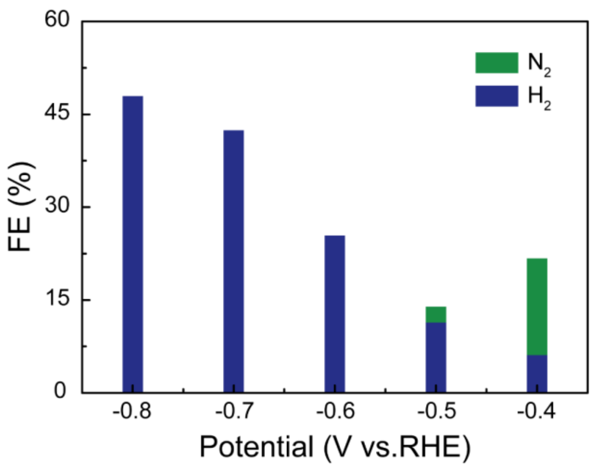

Supplementary Fig. 23| The H_2 and N_2 FE of np/ISAA-CuZn at -0.4 - -0.8 V vs. RHE in 0.2 M $KHCO_3$ + 1 mM KNO_2.

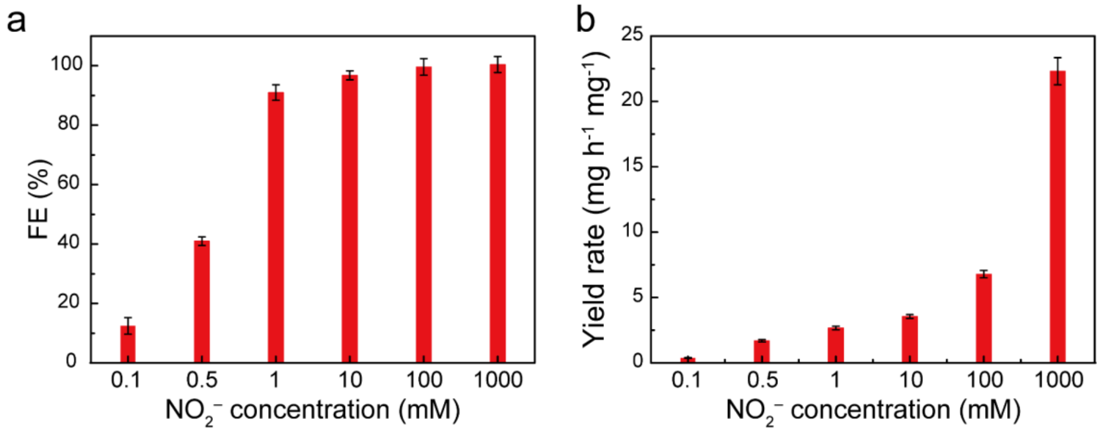

Supplementary Fig. 24| The NH_3 FE(a) and yield rate (b) for np/ISAA-CuZn with concentrations of NO_2^- ranging from 0.1 mM to 1000 mM. The error bands represent the standard deviation of the data obtained from more than three repetitions.

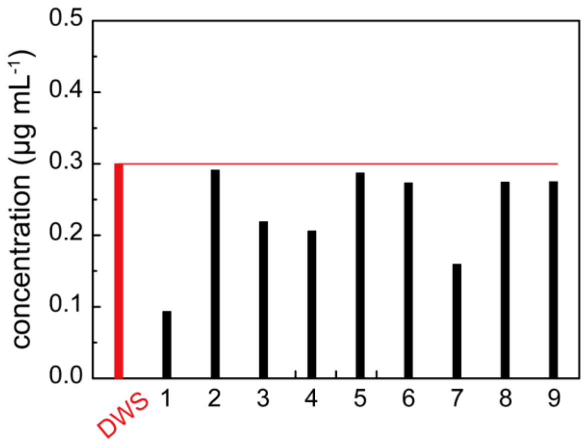

Supplementary Fig. 25| NO_2^--N concentration in solution after MEA test.

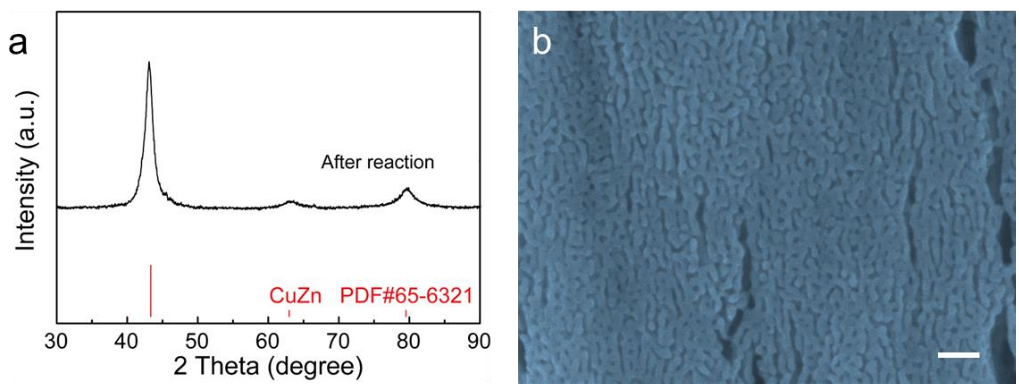

Supplementary Fig. 26| Morphology and composition of np/ISAA-CuZn after MEA test. a, XRD patten. **b,** Cross-section SEM image. Scale bar: 100 nm.

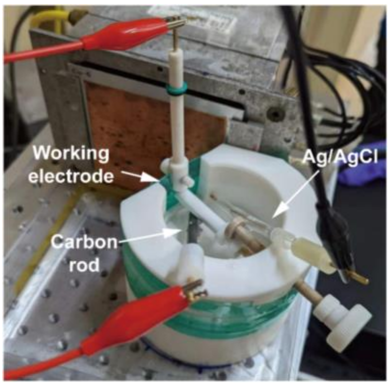

Supplementary Fig. 27| Optical photograph of the tailor-made electrolytic cell used. for in situ XAS characterization.

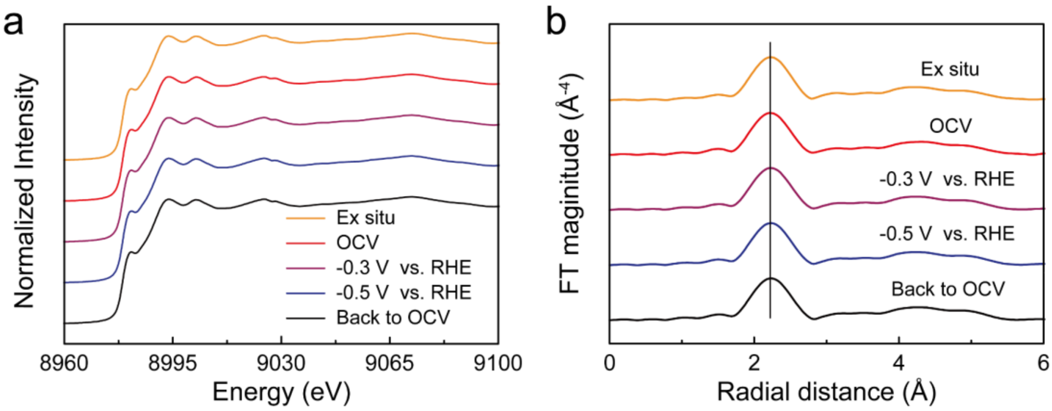

Supplementary Fig. 28| In situ XAS measurements of np/Cu at different applied potentials. In situ XANES spectra (**a**) and FT-EXAFS (**b**) of np/Cu recorded at Cu K-edge.

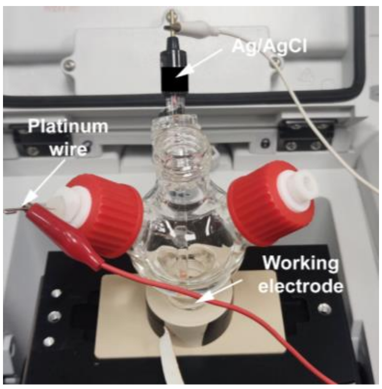

Supplementary Fig.29| Optical photograph of the tailor-made electrolytic cell used. for in situ ATR-SEIRAS characterization.

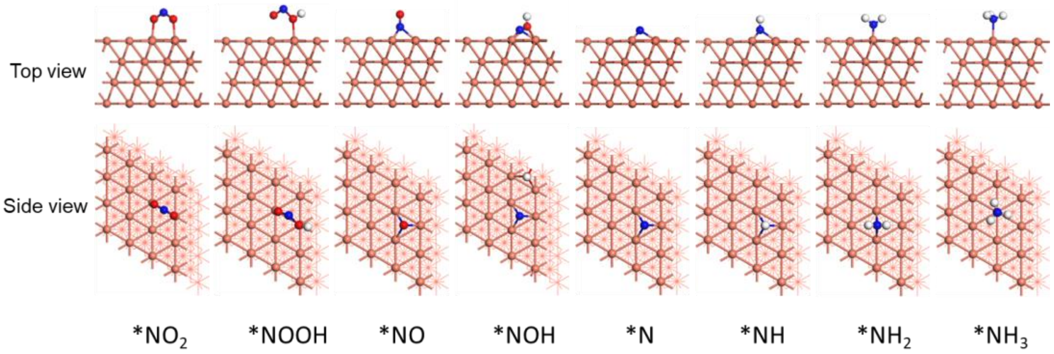

Supplementary Fig. 30| Reaction pathway of the NO_2RR and adsorption models of intermediates on Cu (111) surfaces (Cu: orange, Zn: grey, N: blue, O: red, H: white)

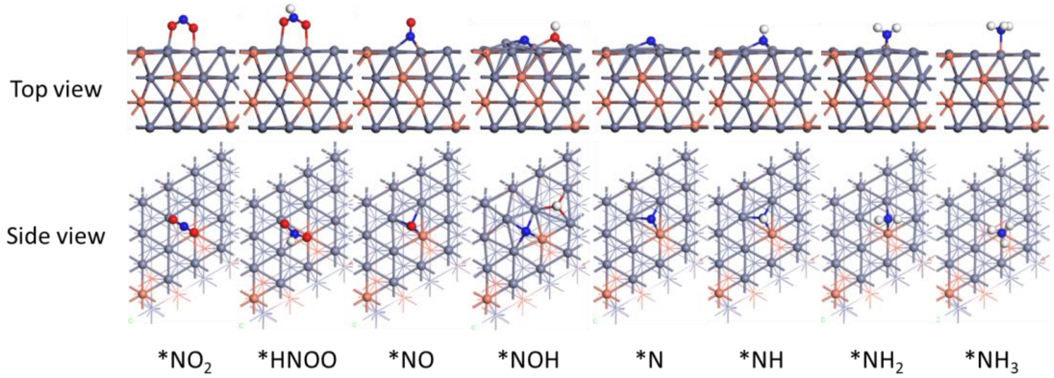

Supplementary Fig. 31| Reaction pathway of the NO_2RR and adsorption models of intermediates on $CuZn_4$ surfaces (Cu: orange, Zn: grey, N: blue, O: red, H: white).

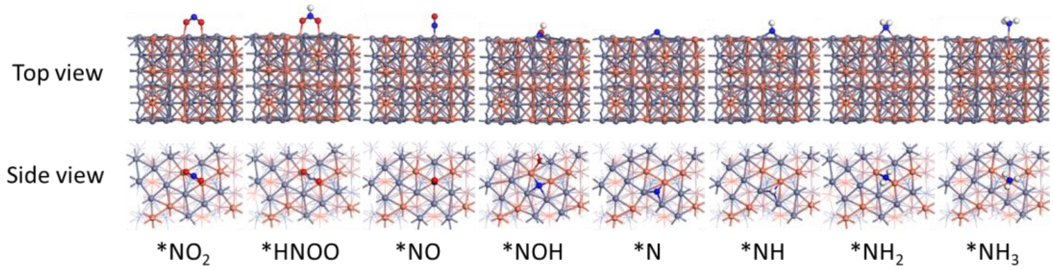

Supplementary Fig. 32| Reaction pathway of the NO_2RR and adsorption models of intermediates on Cu_5Zn_8 surfaces (Cu: orange, Zn: grey, N: blue, O: red, H: white).

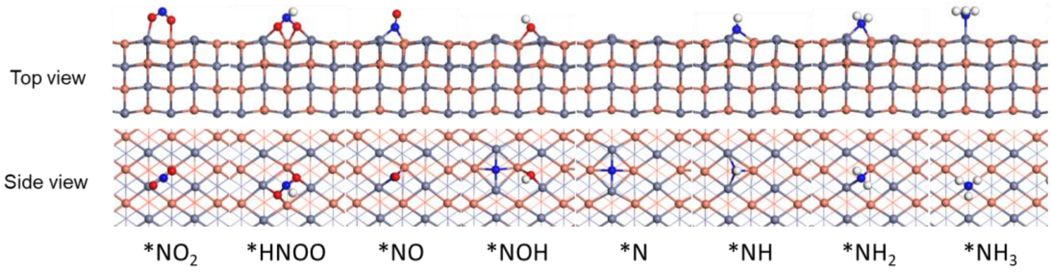

Supplementary Fig. 33| Reaction pathway of the NO2RR and adsorption models of intermediates on ISAA-CuZn surfaces (Cu: orange, Zn: grey, N: blue, O: red, H: white).

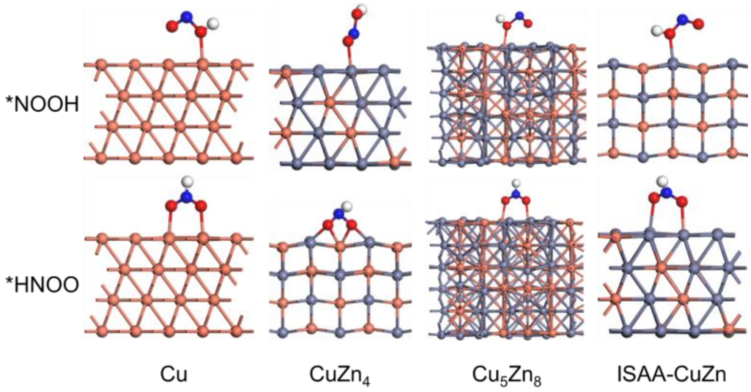

Supplementary Fig. 34| Modelling of adsorption of *NOOH and *HNOO intermediates on Cu, $CuZn_4$, Cu_5Zn_8 and ISAA-CuZn surfaces, respectively.

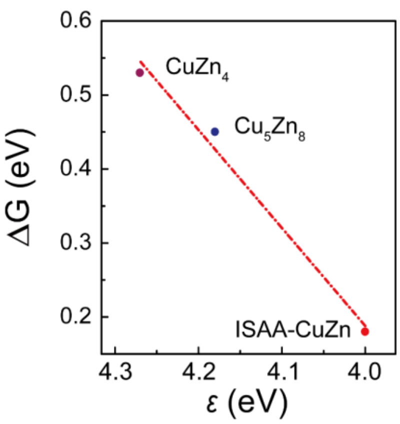

Supplementary Fig. 35| The relationship between computational ε and ΔG of $^*NO_2$ protonation.

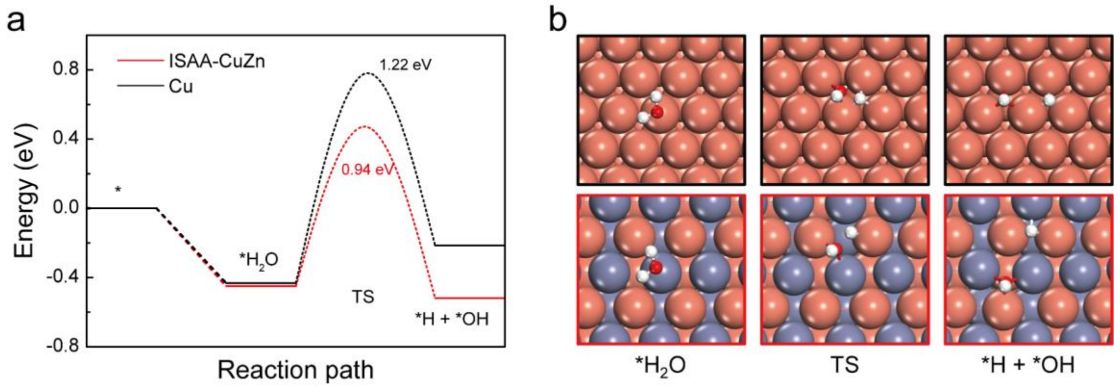

Supplementary Fig. 36| Calculated of the water dissociation step on Cu and np/ISAA-CuZn surfaces. a, Free energy diagrams, **b**, The structure of the *H_2O, transition state (TS), and *H + *OH of the reaction process.

Supplementary Table 1. ICP-OES test result. Elemental composition of np/ISAA-CuZn.

Testing element	Atomic Percentage (%)	Mass percentage (%)
Cu	46.4	45.70
Zn	53.6	54.30

Supplementary Table 2. **EXAFS fitting parameters.** EXAFS fitting parameters at the Cu K-edge and Zn K-edge for np/$CuZn_4$, np/Cu_5Zn_8, np/ISAA-CuZn and refences sample (Cu foil, CuO and Zn foil).

	Samples	Path	*CN*	*R (Å)*	σ^2*(10^{-3} Å^2)*	ΔE_0 *(eV)*	*R-factor*
Cu K-edge	Cu foil	Cu-Cu	12	2.53	8.4	4.2	0.005
	CuO	Cu-O	2.7	1.94	4.2	7.4	0.002
	np/$CuZn_4$	Cu-Zn	7.2	2.63	11.4	2.0	0.02
	np/Cu_5Zn_8	Cu-Cu	1.8	2.54	5.6	5.3	0.07
		Cu-Zn	4.5	2.61	11.8		
	np/ISAA-CuZn	Cu-Zn	4.5	2.54	11.7	10.2	0.013
Zn K-edge	Zn foil	Zn-Zn	8.0	2.66	13.2	0.9	0.012
	np/$CuZn_4$	Zn-Cu	1.8	2.63	14.5	3.0	0.006
		Zn-Zn	8.9	2.64	15.8		
	np/Cu_5Zn_8	Zn-Cu	4.8	2.59	9.8	4.1	0.006
		Zn-Zn	3.0	2.64	12.2		
	np/ISAA-CuZn	Zn-Cu	3.2	2.54	12.3	1.5	0.024

Supplementary Table 3. **Total energy and free energy correction value.** The total energy and free energy correction value of adsorbed NO_2 protonated species over Cu, ISAA-CuZn, Cu_5Zn_8 and $CuZn_4$.

	E_{DFT}	Correction value of G (298.15K, 1 Atm)
ISAA-CuZn*HNOO	-151.54	0.52
ISAA-CuZn*NOOH	-150.99	0.33
Cu*NOOH	-268.85	0.38
Cu*HNOO	-268.80	0.43
Cu_5Zn_8*HNOO	-282.33	0.33
Cu_5Zn_8*NOOH	-282.32	0.35
$CuZn_4$*HNOO	-149.35	0.40
$CuZn_4$*NOOH	-149.29	0.37